Journal of Colloid and Interface Science 351 (2010) 392–397

Contents lists available at ScienceDirect

Journal of Colloid and Interface Science

www.elsevier.com/locate/jcis

Water-soluble ZnO–Au nanocomposite-based probe for enhanced protein detection in a SPR biosensor system

Liying Wang, Ying Sun, Jian Wang, Jing Wang, Aimin Yu, Hanqi Zhang, Daqian Song *

College of Chemistry, Jilin University, Qianjin Street 2699, Changchun 130012, People's Republic of China

ARTICLE INFO

Article history:
Received 27 May 2010
Accepted 20 July 2010
Available online 25 July 2010

Keywords:
Surface plasmon resonance
ZnO–Au nanocomposites
Protein probe
Covalent attachment

ABSTRACT

A surface plasmon resonance biosensor based on ZnO–Au nanocomposites was developed for the detection of rabbit IgG. The ZnO–Au nanocomposites can bind protein by covalent attachment to construct a probe for target analyte. The probe with unique optical properties and good biocompatibility could enhance the sensitivity of SPR biosensor. Under the optimized conditions, the biosensor based on ZnO–Au nanocomposites exhibits a satisfactory response to rabbit IgG in the concentration range of 0.15–20.00 μg ml^{-1}. For comparison, the biosensor based on Au film and the biosensor based on Au nanoparticles were also studied for the detection of rabbit IgG. The biosensor based on Au film shows a response to rabbit IgG in the concentration range of 2.50–20.00 μg ml^{-1}. The biosensor based on Au nanoparticles shows a response in the concentration range of 0.30–20.00 μg ml^{-1}. The biosensor based on ZnO–Au nanocomposites was therefore found to be the most sensitive of the three types of biosensors. The lowest concentration of rabbit IgG that can be determined by the proposed biosensor is about 16-fold lower than that of the biosensor based on Au film alone.

1. Introduction

Zinc oxide has attracted considerable interest because of its unique optical and electrical properties as a typical metal oxide semiconductor [1–3]. ZnO nanocrystals have remarkable characteristics of high surface volume ratio, ease of fabrication, and chemical stability, which have potential applications in many areas, such as drug delivery, chemical and biological sensors, and heterogeneous catalysts [4–6]. ZnO nanocrystals are usually synthesized by the preparation of ZnO sols in the liquid phase from homogeneous ethanolic solutions with precursors of lithium hydroxide and zinc acetate [7,8]. The resulting ZnO nanocrystals have an average diameter ranging from ten to several tens of nanometers. ZnO nanocrystals are unstable in aqueous solution, while biological conjugation usually exists in water solution. In order to satisfy the primary requirement of biological research, the surface of ZnO nanocrystals should be modified.

Recently, metal nanoparticles on the surface of semiconductor nanostructures have become a popular research topic because of the improved optical properties of the semiconductor [9,10]. The surface plasmon resonance electron and energy transfer from the metal surface to the surrounding semiconductor materials significantly modify the optical properties of the metal and the semiconductor [11]. Au nanoparticles were considered as an excellent material to modify semiconductor nanostructures [12]. Au nanoparticles have been used widely in self-assembly, biolabeling, immunoassays, electron-transfer theories, and crystal growth [13,14]. When ZnO nanocrystals were modified with Au nanoparticles, ZnO–Au nanocomposites were stable in the aqueous phase and used as a probe to detect biomolecules. Recently, several papers have reported the synthesis and optical properties of the heterostructured ZnO–Au nanocomposites [15–18]. Thiol-oligonucleotide DNA labeled with ZnO–Au nanocomposites by Au–S covalent bonds has a strong Raman signal and it is a novel method for identifying DNA microarrays [17]. Through binding the ZnO–Au nanoparticles to protein by electrostatic interactions, a new method for detecting protein was explored on the resonant Raman scattering signal [19].

Surface plasmon resonance (SPR) biosensor is a powerful tool because of its characteristics of label-free detection and small sample volume and it can be performed in real time [20]. These characteristics make the SPR technique an easy, convenient, and reliable one for studying molecular recognition processes of kinetics constants and binding specificity of individual biomolecules. To enhance the sensitivity, most of the sensor designs are concerned with surface modifications, such as SPR chips coated with dextran to increase the loading of biomolecules, or employ liposomes, Ag film, or Au nanoparticles [21–23]. As an excellent protein carrier, Au nanoparticles play an important role in enhancing the sensitivity of SPR biosensors. Generally, two approaches are used to apply the Au nanoparticles in SPR biosensors. One approach is that the Au nanoparticles are adsorbed onto the self-assembled monolayer

* Corresponding author. Fax: +86 431 85112355.
E-mail address: songdq@jlu.edu.cn (D. Song).

0021-9797/$ - see front matter © 2010 Elsevier Inc. All rights reserved.
doi:10.1016/j.jcis.2010.07.050

of thiol or dithiol formed on the SPR biosensor [24]. The other is that Au nanoparticles couple with antigen and Au–antigen binds to the antibody immobilized on the SPR biosensor [25]. ZnO–Au nanocomposites were used to modify a SPR biosensor chip by a self-assembly technique in our previous work [26]. Here, instead of immobilization of ZnO–Au nanocomposites on the SPR biosensor chip directly, ZnO–Au nanocomposites were used to couple with antigen to construct the protein probe. Due to the unique optical properties and good biocompatibility, the probe could be used to enhance the sensitivity of the SPR biosensor.

In this paper, water-soluble ZnO–Au nanocomposites were successfully synthesized [15]. In order to enhance the sensitivity of the SPR biosensor, it is important to construct a protein probe modified with ZnO–Au nanocomposites. The ZnO–Au nanocomposites can bind protein by covalent attachment to construct a protein probe. Here 3-mercaptopropionic acid (MPA) was used to connect the Au nanoparticles in ZnO–Au nanocomposites as a strong, specific interaction between the thiol–gold interactions [27]. After the carboxyl group of MPA was activated, ZnO–Au nanocomposites could bind to antigen. When the ZnO–Au antigen interacts with antibody immobilized on the SPR biosensor, the bindings of ZnO–Au–protein–protein lead to changes in the refractive index at the sensor surface. The changes result in a shift of resonant wavelength which can be easily measured by the SPR biosensor.

2. Materials and methods

2.1. Reagents

Rabbit IgG, goat anti-rabbit IgG and human IgM were purchased from Beijing Biosynthesis Biotechnology Company. 3-Mercaptopropionic acid was purchased from Jkchemical. *N*-hydroxysuccinimide (NHS) and 1-ethyl-3-(3-dimethylaminopropyl)carbodiimide (EDC) were purchased from Pierce. Bovine serum albumin (BSA) was purchased from Beijing Ding Guo Biotechnology Company. Hydrogen tetrachloroauratehydrate, trisodium citrate, zinc acetate dehydrate, lithium hydroxide monohydrate, ethanol, and all other chemicals were of analytical reagent grade. All solutions were prepared with ultrapure water. Rabbit IgG, goat anti-rabbit IgG, and human IgM were stored at −20 °C. Sodium phosphate-buffered saline (PBS, 0.01 mol L^{-1}, pH 7.4) was used as running buffer.

2.2. Equipment

The wavelength modulation SPR biosensor installed in our laboratory was used. It is working with a Kretschmann configuration to achieve the resonant conditions by attenuated total reflection in a prism. A K9 glass slide was used and a 2-nm adhesive layer of Cr followed by a 50-nm layer of Au was deposited on the glass slide. The glass slide with Au film was put on base of a prism (K9 glass) using a suitable index matching oil (cedar oil). A halogen tungsten lamp was used as the excitation light source. The light from this source passes through a polarizer and two lenses and becomes TM-polarized parallel light. The parallel polychromatic light beam passes through the optical prism and excites surface plasmon at the interface between the Au film and the analyte. The output light is guided into the optical fiber and then enters the full wavelength spectrophotometer (Ocean Optics, Inc., USA). A 100-μl volume flow cell was used. The interaction between the analyte in the solution and the biomolecular element immobilized on the SPR biosensor produces a change in refractive index that is observed as a shift in the SPR resonant wavelength.

2.3. Procedures

2.3.1. Preparation of water-soluble ZnO–Au nanocomposites

Water-soluble ZnO–Au nanocomposites were prepared according to the method reported [15]. Briefly, 50 ml of ethanol containing 1.10 g zinc acetate dihydrate was refluxed while stirring at about 80 °C for 100 min and the precursor solution was obtained. Then the precursor was hydrolyzed by adding 50 ml of ethanol containing 0.29 g lithium hydroxide monohydrate in an ultrasonic bath at 0 °C for 30 min. The resultant in 6 ml of ZnO nanocrystals solution was precipitated and then redispersed in 30 ml of 3.0 mmol L^{-1} trisodium citrate solution with the aid of ultrasound. After that 20 ml of 0.5 mmol L^{-1} $HAuCl_4$ solution was added while vigorously stirring at room temperature for 48 h. The color of the solution changed from pale yellow to purple and the ZnO–Au nanocomposites homogeneously dispersed in aqueous solution. For comparison, Au nanoparticles were also prepared via the same method of trisodium citrate reduction of $HAuCl_4$ in water following a known method [28].

2.3.2. Immobilization of antibody

The glass slide with Au film was fixed under the flow cell. After PBS was injected into the flow cell as the baseline solution, 10 mmol L^{-1} MPA was injected into the flow cell. Then the biosensor surface was activated with NHS (30 mg ml^{-1}) under the catalysis of EDC (30 mg ml^{-1}) for 20 min. The goat anti-rabbit IgG was injected into the flow cell. After 12 h, PBS buffer was injected into the flow cell to wash off noncovalently bound antibody and to stabilize the baseline. Prior to the analysis, 1 mol L^{-1} ethanolamine hydrochloride (pH 8.0) was injected into the flow cell to block the nonspecific binding sites on the biosensor surface for 10 min. Schematic illustration of antibody immobilization on the SPR biosensor surface is shown in Fig. 1a.

2.3.3. Preparation of ZnO–Au nanocomposites coupled with antigen

Twenty microliters of MPA (pH 7.0, adjusted by sodium hydroxide solution) was added into 20 ml of ZnO–Au nanocomposites solution and incubated for 24 h. Then 0.4 ml of NHS (100 mg ml^{-1}) and 0.4 ml of EDC (100 mg ml^{-1}) were added into the solution. The carboxyl group of MPA was activated with NHS under the catalysis of EDC for 20 min. The conjugates were then centrifuged at 15,000*g* for 30 min. The precipitate was redispersed in PBS buffer solution. The ZnO–Au–protein was prepared by adding rabbit IgG to the redispersed ZnO–Au nanocomposites solution and incubating for 45 min at 4 °C. Different ratios between rabbit IgG and ZnO–Au nanocomposites were used to select the optimum experimental conditions. Then 10 μl of 10 mg ml^{-1} BSA was added to 1 ml ZnO–Au–protein solution to block the nonspecific binding sites. The process of the ZnO–Au nanocomposites coupled with antigen is illustrated in Fig. 1b.

For comparison, Au–protein probes were also prepared by adding rabbit IgG to Au nanoparticle solution and incubating for 45 min at 4 °C [25,29,30]. The conjugates were then centrifuged at 12,500*g* for 20 min. The precipitate was redispersed in PBS buffer solution.

2.3.4. Immunoassay

At room temperature, different concentrations of ZnO–Au–IgG diluted with PBS buffer were separately injected into the flow cell over the immobilized antibody surface. The interaction between rabbit IgG in the solution and the goat anti-rabbit IgG immobilized on the SPR biosensor surface produces a change in the refractive index that is observed as the shift of the SPR resonant wavelength. Then PBS buffer was injected into the flow cell. When the antigen was dissociated from the antibody on the biosensor surface,

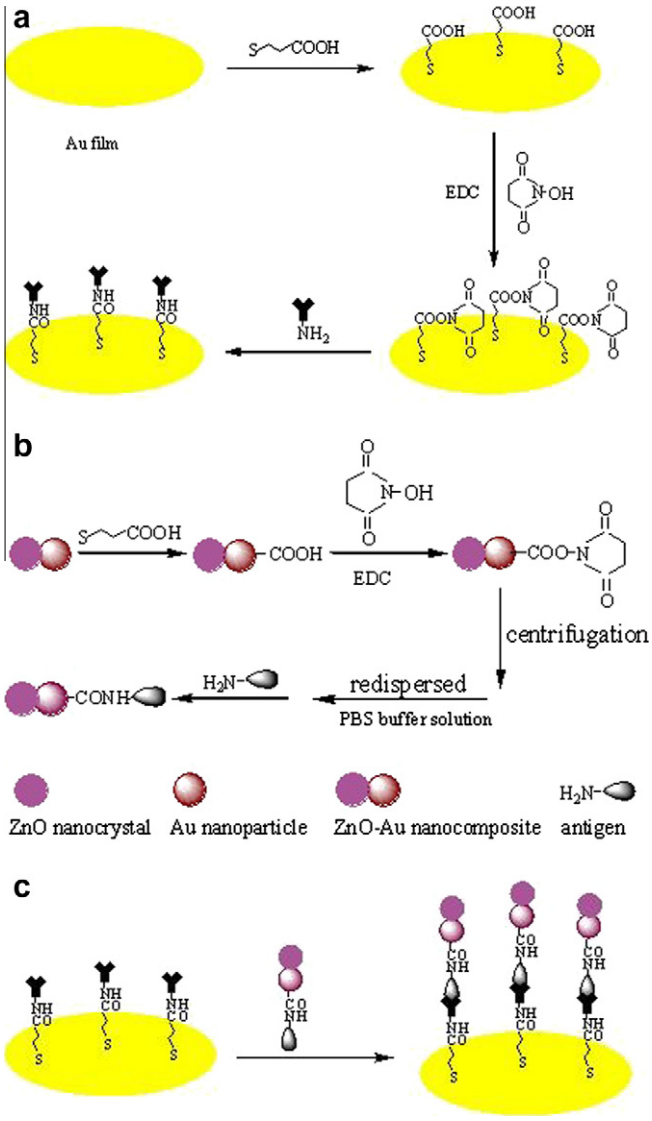

Fig. 1. Schematic illustrations of immobilization of antibody (a), ZnO–Au nanocomposites coupling to antigen (b), and immunoassay (c); (Υ_{NH_2}) antibody.

another sample was injected into the flow cell. Schematic illustration of the immunoassay is shown in Fig. 1c.

For comparison, different concentrations of rabbit IgG and different concentrations of Au–IgG diluted with PBS buffer were also separately injected into the flow cell. The detection procedures were the same as those noted above.

To evaluate the selective binding of rabbit IgG, ZnO–Au–BSA and human IgM were determined by the same procedure as that used to determine rabbit IgG.

3. Results and discussion

3.1. Characterization of ZnO–Au nanocomposites

The transmission electron microscope (TEM) images of the synthesized ZnO nanocrystals, Au nanoparticles, and ZnO–Au nanocomposites are shown in Fig. 2. The morphologies of ZnO nanocrystals and Au nanoparticles are shown in Fig. 2a and b. Their average sizes were about 6 and 23 nm, respectively. It can be seen from Fig. 2c and d that the average size of the ZnO–Au nanocomposites was about 10 nm. The ZnO nanocrystals were unstable in aqueous solution and they could be precipitated by adding water due to the weak interaction of surface ligand and water [17]. However, after linking with Au nanoparticle, ZnO–Au nanocomposites were stable in the aqueous phase, which further confirmed that ZnO–Au nanocomposites were synthesized successfully. UV–vis spectrum for the Au nanoparticles and ZnO–Au nanocomposites is shown in Fig. 3. The absorption values of Au nanoparticles and ZnO–Au nanocomposites in water are centered at 520 and 546 nm, respectively [26]. The red shift of the surface plasmon spectrum of the ZnO–Au nanocomposites is due to the strong interfacial coupling between Au and ZnO. The transfer of electrons from Au to ZnO occurs until two systems reach equilibrium.

3.2. Immobilization of goat anti-rabbit IgG

The SPR sensor chip surface is usually coated with sulfhydryl compounds and the receptor molecules could be covalently immobilized for specific analyte capture. After the glass slide with Au film was fixed under the flow cell, PBS was injected into the flow cell as the baseline solution. Then MPA was injected into the flow cell to react with the Au film. The formation of monolayers is driven by a strong, specific interaction between the thiol and the metal surface. After PBS was injected into the flow cell, the maximum shift of the resonant wavelength for the formation of this monolayer is 7.13 nm, which indicates that a MPA monolayer was formed on the Au film. NHS and EDC are usually used for the surface activation. NHS reacted with MPA under the catalysis of EDC. In order to make every carboxyl group immobilized on the Au film be activated, excess amounts of EDC and NHS were used. The amounts are not dependent on the quantities of proteins used further. The surplus NHS and EDC were removed by injecting PBS buffer to the flow cell. After the biosensor surface was activated, the goat anti-rabbit IgG diluted with PBS buffer was injected into the flow cell to perform its binding on the activated surface. The covalent attachment between the amine group and the carboxyl group is a good stratagem for the immobilization of antibody on the Au film. The assembling curve of antibody on the sensor surface is shown in Fig. 4. It can be seen that goat anti-rabbit IgG sensing membrane formed well within 1 h. The maximum resonant wavelength shift for the immobilization of goat anti-rabbit IgG is 13.74 nm within 100 min.

In order to select the optimum concentration of antibody, different concentrations of goat anti-rabbit IgG were used to form the sensing layer. The effects of the concentration of goat anti-rabbit IgG on the shift of the resonant wavelength are also shown in Fig. 4. It can be seen that the resonant wavelength shows an evident shift at first and then changes slowly with an increase of the time. With the increase of the concentration, more antibodies were immobilized on the sensor surface. While the concentration further increased, the antibody immobilized on the surface reached saturation, which resulted in a slight change of the resonant wavelength and the noncovalent binding of antibody was increased. After 12 h, PBS buffer was injected into the flow cell to wash off noncovalent binding of antibody; the maximum resonant wavelength shifts for the immobilization of goat anti-rabbit IgG at concentrations of 75 and 100 μg ml^{-1} are almost the same. As a result, 75 μg ml^{-1} was chosen as the optimum concentration of goat anti-rabbit IgG for the detection of rabbit IgG. As shown in Fig. 4d, when the concentration of goat anti-rabbit IgG is 75 μg ml^{-1}, the shift of the resonant wavelength reached about 88% of its total shift within 1 h. The maximum resonant wavelength shift for the immobilization of goat anti-rabbit IgG is 12.73 nm within 100 min.

3.3. ZnO–Au nanocomposites coupled with antigen

MPA was added to ZnO–Au nanocomposite solution and the thiol terminal groups were able to bind stably with Au nanoparticles.

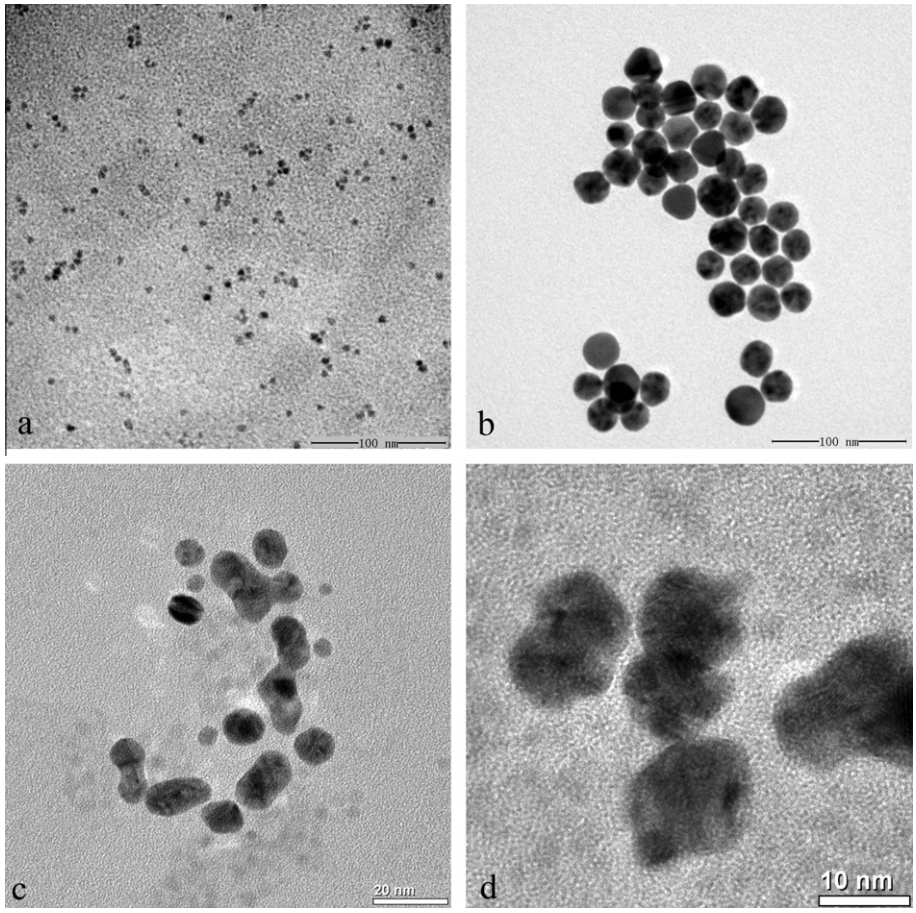

Fig. 2. Transmission electron microscope (TEM) images of ZnO nanocrystals (a), Au nanoparticles (b), ZnO–Au nanocomposites (c), and high-resolution images of ZnO–Au nanocomposites (d).

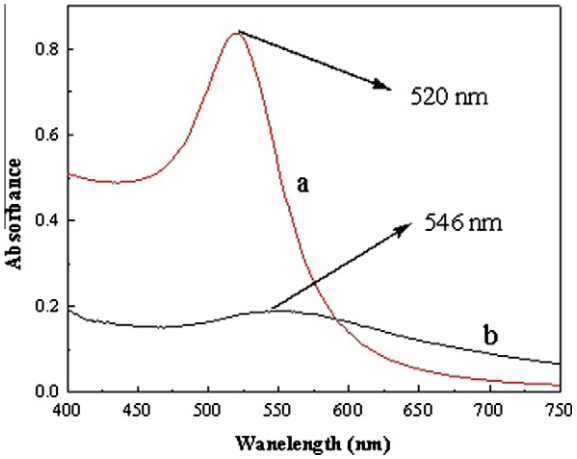

Fig. 3. UV–vis absorption spectra of Au nanoparticles (a) and ZnO–Au nanocomposites (b).

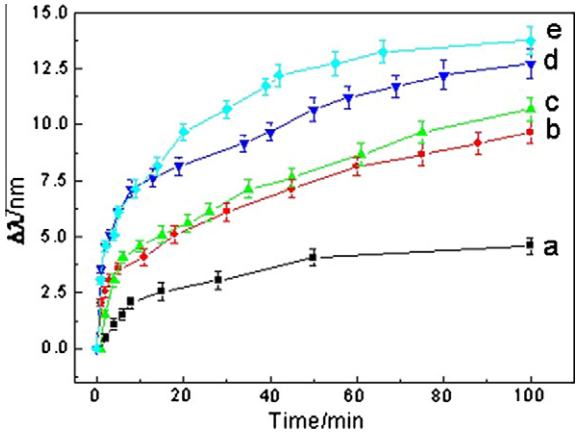

Fig. 4. Kinetic assembling curves of goat anti-rabbit IgG on the MPA monolayer. The concentration of goat anti-rabbit IgG: (a) 12.5 μg ml^{-1}, (b) 25 μg ml^{-1}, (c) 50 μg ml^{-1}, (d) 75 μg ml^{-1}, (e) 100 μg ml^{-1}.

Compared with the amount of MPA, excess amounts of NHS and EDC were used to make every carboxyl group be activated completely. After the carboxyl group of MPA was activated with NHS under the catalysis of EDC, the conjugates were centrifuged to remove the impurities and then the precipitate was redispersed in PBS solution. Then the ZnO–Au–protein probe was prepared with the addition of rabbit IgG to the ZnO–Au nanocomposite solution. In theory, the protein can be adsorbed directly on the Au nanoparticles, while the attachment between Au nanoparticles and protein is weaker compared with covalent attachment between carboxyl group and amine group [30,31]. As a result, covalent attachment was applied to construct the ZnO–Au–protein probe in this study. When NHS and EDC were added into Au nanocomposite solution, the sol color changed into blue immediately. Au nanoparticles linked with ZnO nanocrystals may prevent the Au nanoparticles from coagulation when NHS and EDC were added.

3.4. The selection of ratio between rabbit IgG and ZnO–Au nanocomposites

Twenty milliliters of ZnO–Au nanocomposite solution was centrifuged and redispersed in 8 ml PBS solution. Then 5 μg of rabbit IgG was separately added into 0.0625, 0.125, 0.25, 0.5, and 1 ml redispersed ZnO–Au nanocomposite solution and the solutions were diluted with PBS buffer to 1 ml. After 40 min, 10 μl of 10 mg ml^{-1} BSA was added into ZnO–Au–protein solution to block the nonbinding sites. Then the solution containing 5 μg rabbit IgG and different concentrations of ZnO–Au nanocomposites was separately injected into the flow cell to evaluate the effect of the volume of ZnO–Au nanocomposite solution. Fig. 5 shows the effect of the volume of ZnO–Au nanocomposites solution. It can be seen from Fig. 5 that the shift of resonant wavelength significantly increases when the volume of ZnO–Au nanocomposite solution increases from 0 to 0.25 ml and slightly increases when the volume of ZnO–Au nanocomposites solution increases from 0.25 to 1 ml. The SPR response signal increases with the amount of ZnO–Au–protein modified on the surface of the biosensor and then levels off. As a result, 0.25 ml ZnO–Au nanocomposites solution was selected as the optimum volume to connect with 5 μg rabbit IgG.

3.5. Determination of rabbit IgG

At room temperature, after goat anti-rabbit IgG was immobilized on the surface of the biosensor, rabbit IgG at different concentrations was separately injected into the flow cell. The shifts of resonant wavelength due to antibody–antigen immunoreactions were measured. For the traditional assay (the IgG without labeled), the rabbit IgG was diluted with PBS to obtain different concentration solutions. Fig. 6a shows the relationship between the shifts in the resonant wavelength and the concentrations of rabbit IgG. The minimum shift of resonant wavelength is 0.51 nm at 2.50 μg ml^{-1} and the maximum shift of resonant wavelength is 2.54 nm at 20.00 μg ml^{-1}.

For the Au nanoparticles assay, Au–IgG was diluted with PBS to obtain different concentration solutions. Fig. 6b shows the relationship between the shifts in the resonant wavelength and the concentrations of rabbit IgG. The minimum shift of resonant wavelength is 0.51 nm at 0.30 μg ml^{-1} and the maximum shift of resonant wavelength is 5.08 nm at 20.00 μg ml^{-1}.

For the ZnO–Au nanocomposite-enhanced assay, 0.25 ml ZnO–Au nanocomposite solution was selected as the optimum volume to connect 5 μg rabbit IgG. Therefore, 20 μg rabbit IgG was added to 1 ml ZnO–Au nanocomposite solution and ZnO–Au–IgG solutions with different concentrations were diluted with PBS buffer. After 40 min, 10 μl of 10 mg ml^{-1} BSA was added to ZnO–Au–IgG solution to block the nonbinding sites of Au nanoparticles in the ZnO–Au nanocomposites and also to avoid interaction between Au nanoparticles and antibody. Then solutions containing of ZnO–Au–IgG at different concentrations were separately injected into the flow cell. Fig. 6c shows the relationship between the shifts in the resonant wavelength and the concentrations of rabbit IgG. When the rabbit IgG was modified with ZnO–Au nanocomposites, the minimum shift of resonant wavelength is 0.51 nm at 0.15 μg ml^{-1} and the maximum shift of resonant wavelength is 6.08 nm at 20.00 μg ml^{-1}.

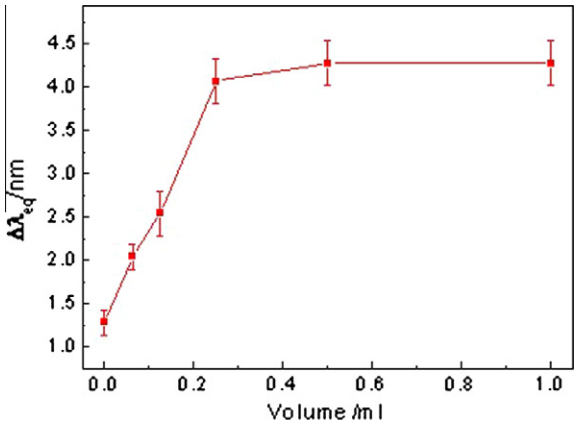

Fig. 5. The relationship between the different volumes of ZnO–Au nanocomposite solutions and the shifts of resonant wavelength due to antibody–antigen immunoreactions. The amount of rabbit IgG is 5 μg.

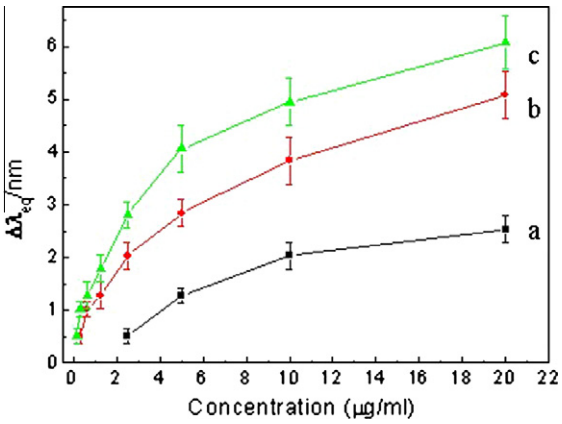

Fig. 6. The relationship between the concentration of rabbit IgG and the shift in the resonant wavelength $\Delta\lambda_{eq}$. (a) The biosensor based on Au film, (b) the biosensor based on Au nanoparticles, and (c) the biosensor based on ZnO–Au nanocomposites.

It can be seen clearly from Fig. 6 that the biosensor based on Au film shows a response to rabbit IgG in the concentration range of 2.50–20.00 μg ml^{-1}. The biosensor based on Au nanoparticles shows a response to rabbit IgG in the concentration range of 0.30–20.00 μg ml^{-1}. The biosensor based on ZnO–Au nanocomposites shows a response to rabbit IgG in the concentration range of 0.15–20.00 μg ml^{-1}.

When the rabbit IgG was modified with ZnO–Au nanocomposites, the lowest concentration determined by the SPR biosensor is lower than those obtained by the SPR biosensor based on Au film and the biosensor based on Au nanoparticles. A significant increase in sensitivity is therefore obtained through the use of ZnO–Au nanocomposites in SPR biosensors. The surface plasmon of the Au nanoparticles might be resonantly excited through energy transfer in the near field and create a strong local electromagnetic field [32,33]. The incident light field coupling to the local surface plasmon field might induce a strong localized electromagnetic field in the ZnO–Au nanocomposites, which further enhances the shift of resonant wavelength. On the other hand, when the ZnO–Au nanocomposites couple with antigen, the sizes of the IgG increase and produce a change in refractive index that is observed as a shift in the SPR resonant wavelength. Due to the two factors, the limit of determination for rabbit IgG obtained by the biosensor based on ZnO–Au nanocomposites was lower than that obtained by the biosensor based on Au film. The sensitivity of the biosensor was significantly enhanced. Meanwhile, this biosensor extended the application of ZnO–Au nanocomposites in immunoassay.

3.6. Interference experiments

After the goat anti-rabbit IgG was immobilized on the surface of the biosensor, 1 ml of ZnO–Au nanocomposite solution containing

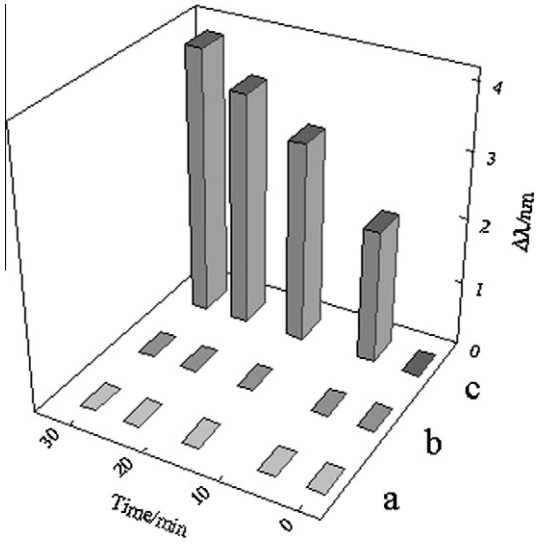

Fig. 7. Kinetic assembling curves of ZnO–Au–BSA (a), human IgM (b), and rabbit ZnO–Au–IgG (c).

100 μg ml^{-1} BSA and 1 ml of 10 μg ml^{-1} human IgM were separately injected into the flow cell for 30 min and the experimental results are shown in Fig. 7a and b, respectively. There are no observable shifts of the resonant wavelength, which indicated that the ZnO–Au–BSA and human IgM do not interact with antibody immobilized on the biosensor surface.

For comparison, the solution containing ZnO–Au–IgG (5 μg ml^{-1}) was injected into the flow cell. The kinetic assembling curve due to antibody–antigen interaction is shown in Fig. 7c. The experimental results indicated that the nonspecific binding was not observed.

4. Conclusion

The sensitivity enhancement of SPR biosensors to detect rabbit IgG based on ZnO–Au nanocomposites was studied. A ZnO–Au–protein probe was constructed by covalent attachment. When the concentration of goat anti-rabbit IgG is 75 μg ml^{-1}, the biosensor based on ZnO–Au nanocomposites exhibits a response in the concentration range of 0.15–20.00 μg ml^{-1}. The lowest concentration of the rabbit IgG that could be detected with the proposed biosensor is lower than the biosensor based on Au film and the biosensor based on Au nanoparticles. The ZnO–Au–protein probe can be used to enhance the sensitivity of the biosensor significantly for the determination of rabbit IgG.

Acknowledgments

This work was supported by National Natural Science Foundation of China (No. 20727003) and Science and Technology Developing Foundation of Jilin Province (No. 20070551).

References

[1] C. Soci, A. Zhang, B. Xiang, S.A. Dayeh, D.P.R. Aplin, J. Park, X.Y. Bao, Y.H. Lo, D. Wang, Nano Lett. 7 (2007) 1003–1009.
[2] C.S. Lao, J. Liu, P.X. Gao, L.Y. Zhang, D. Davidovic, R. Tummala, Z.L. Wang, Nano Lett. 6 (2006) 263–266.
[3] H.B. Zeng, W.P. Cai, P.S. Liu, X.X. Xu, H.J. Zhou, C. Klingshirn, H. Kalt, ACS Nano 2 (2008) 1661–1670.
[4] Z.L. Wang, Annu. Rev. Phys. Chem. 55 (2004) 159–196.
[5] C.L. Kuo, T.J. Kuo, M.H. Huang, J. Phys. Chem. B 109 (2005) 20115–20121.
[6] H.H. Wang, C. Xie, J. Cryst. Growth 291 (2006) 187–195.
[7] L. Spanhel, M.A. Anderson, J. Am. Chem. Soc. 113 (1991) 2826–2833.
[8] Q.F. Zhang, C.S. Dandeneau, X.Y. Zhou, G.Z. Cao, Adv. Mater. 21 (2009) 1–22.
[9] M. Fukusima, N. Managaki, M. Fujii, H. Yanagi, S. Hayashi, J. Appl. Phys. 98 (2005) 024316-1–024316-4.
[10] N.E. Hecker, R.A. Höfel, N. Sawaki, T. Maier, G. Stasser, Appl. Phys. Lett. 75 (1999) 1577–1579.
[11] G.H. Ma, J. He, K. Rajiv, S.H. Tang, Y. Yang, M. Nogami, Appl. Phys. Lett. 84 (2004) 4684–4686.
[12] F.R. Fan, Y. Ding, D.Y. Liu, Z.Q. Tian, Z.L. Wang, J. Am. Chem. Soc. 131 (2009) 12036–12037.
[13] M.C. Daniel, D. Astruc, Chem. Rev. 104 (2004) 293–346.
[14] Y.W. Cao, R.C. Jin, C.A. Mirkin, J. Am. Chem. Soc. 123 (2001) 7961–7962.
[15] X. Wang, X. Kong, Y. Yu, H. Zhang, J. Phys. Chem. C 111 (2007) 3836–3841.
[16] G.Y. Shan, M.Y. Zhong, S. Wang, Y.J. Li, Y.C. Liu, J. Colloid Interface Sci. 326 (2008) 392–395.
[17] Y.C. Liu, M.Y. Zhong, G.Y. Shan, Y.J. Li, B.Q. Huang, G.L. Yang, J. Phys. Chem. B 112 (2008) 6484–6489.
[18] M.K. Lee, T.G. Kim, W. Kim, Y.M. Sung, J. Phys. Chem. C 112 (2008) 10079–10082.
[19] G.Y. Shan, S. Wang, X.F. Fei, Y.C. Liu, G.L. Yang, J. Phys. Chem. B 113 (2009) 1468–1472.
[20] J. Homola, S.S. Yee, G. Gauglitz, Sens. Actuators B 54 (1999) 3–15.
[21] L.A. Lyon, D.J. Peña, M.J. Natan, J. Phys. Chem. B 103 (1999) 5826–5831.
[22] L.Y. Wang, Y. Sun, J. Wang, X.N. Zhu, F. Jia, Y.B. Cao, X.H. Wang, H.Q. Zhang, D.Q. Song, Talanta 78 (2009) 265–269.
[23] T. Kawaguchi, D.R. Shankaran, S.J. Kim, K. Matsumoto, K. Toko, N. Miura, Sens. Actuators B 133 (2008) 467–472.
[24] E. Hutter, J.H. Fendler, D. Roy, J. Phys. Chem. B 105 (2001) 11159–11168.
[25] X. Liu, Y. Sun, D.Q. Song, Q.L. Zhang, Y. Tian, S.Y. Bi, H.Q. Zhang, Anal. Biochem. 333 (2004) 99–104.
[26] L.Y. Wang, J. Wang, S.L. Zhang, Y. Sun, X.N. Zhu, Y.B. Cao, X.H. Wang, H.Q. Zhang, D.Q. Song, Anal. Chim. Acta 653 (2009) 109–115.
[27] T.Y.B. Leung, M.C. Gerstenberg, D.J. Lavrich, G. Scoles, F. Schreiber, G.E. Poirier, Langmuir 16 (2000) 549–561.
[28] J. Turkevitch, P.C. Stevenson, J. Hillier, Discuss. Faraday Soc. 11 (1951) 55–75.
[29] P. Englebienne, Analyst 123 (1998) 1599–1603.
[30] L.A. Lyon, M.D. Musick, M.J. Natan, Anal. Chem. 70 (1998) 5177–5183.
[31] Z.K. Amir, A.A. Dhirani, Chem. Rev. 108 (2008) 4072–4124.
[32] K. Okamoto, I. Niki, A. Shvartser, Y. Narukawa, T. Mukai, A. Scherer, Nat. Mater. 3 (2004) 601–605.
[33] J.H. Song, T. Atay, S. Shi, H. Urabe, A.V. Nurmkko, Nano Lett. 5 (2005) 1557–1561.